

# Oceanography, primary production and dissolved inorganic nitrogen uptake in two Leeuwin Current eddies

A.M. Waite<sup>a,\*</sup>, S. Pesant<sup>a,c</sup>, D.A. Griffin<sup>b</sup>, P.A. Thompson<sup>b</sup>, C.M. Holl<sup>d,e</sup>

<sup>a</sup>*School of Environmental Systems Engineering, University of Western Australia, Crawley 6009, WA, Australia*

<sup>b</sup>*Marine and Atmospheric Research, Commonwealth Scientific and Industrial Research Organization, Hobart, TAS, Australia*

<sup>c</sup>*Laboratoire d'Océanographie de Villefranche, CNRS– Université Pierre et Marie Curie–Paris 6, 06230 Villefranche-sur-Mer, France*

<sup>d</sup>*School of Biology, Georgia Institute of Technology, Atlanta, GA, USA*

<sup>e</sup>*Oceanic Institute, 41-202 Kalaniana'ole Highway, Waimanalo, HI 96795, USA*

Accepted 25 March 2007

Available online 29 June 2007

## Abstract

The Leeuwin Current (LC) is an unusual poleward-flowing eastern boundary current that carries warm, low-salinity water southward along the coast of Western Australia. LC dynamics include the formation of a dynamic mesoscale eddy field whose biological dynamics have not been studied. Satellite altimetry indicates that the eddies studied in the 2003 field programme were dynamically typical of LC eddies, but the warm-core (WC) eddy was relatively large and long-lived. The WC eddy contained relatively elevated chlorophyll *a* concentrations thought to originate, at least in part, from the continental shelf/shelf break region and to have been incorporated during eddy formation. Primary production per unit volume in the WC eddy was  $\sim 2 \times$  higher than in the cold-core (CC) eddy due to an historical accumulation of chlorophyll *a* over the period since eddy formation (5–6 months), though chlorophyll *a*-specific daily production was volumetrically  $\sim 50\%$  greater in the CC eddy. In the WC eddy, nitrate uptake rates were  $4 \times$  greater than in the CC eddy, despite the fact that vertical diffusive fluxes of nitrate into the WC eddy were probably only 50% of those in the CC eddy. We therefore hypothesize that other nitrate sources were important, possibly including isopycnal mixing and/or lateral transport into the eddy from surrounding waters. In addition, a deep mixed layer favoured a large ( $> 5 \mu\text{m}$ ) diatom population within the centre of the WC eddy while the CC eddy was persistently stratified, with a shallower mean mixed-layer depth ( $\sim 100 \text{ m}$  vs.  $\sim 200 \text{ m}$  for the WC eddy) and a well developed deep chlorophyll *a* maximum at  $\sim 100 \text{ m}$  composed of 30% prochlorophytes (not capable of taking up nitrate). Both factors probably contributed to higher *f*-ratios in the WC and in the  $> 5 \mu\text{m}$  phytoplankton relative to total phytoplankton.

© 2007 Elsevier Ltd. All rights reserved.

**Keywords:** Primary production; Nutrient uptake; Eddy; Leeuwin Current; *f*-ratio; Mixed-layer depth

## 1. Introduction

The presence of mesoscale (50–200 km diameter) cyclonic eddies can have a significant impact on regional nutrient dynamics, strongly impacting primary production (McGillicuddy and Robinson, 1997; Letelier et al., 2000; Garçon et al., 2001).

\*Corresponding author. Tel.: +61 8 6 3082;  
fax: +61 8 9380 1015.

E-mail address: [Anya.Waite@uwa.edu.au](mailto:Anya.Waite@uwa.edu.au) (A.M. Waite).

Globally, mesoscale eddies have been seen to generate large productivity pulses in many nutrient-poor regions of the world's oceans (Letelier et al., 2000; Garçon et al., 2001) by two primary mechanisms: “eddy pumping” of nutrients upwards from deep to shallow waters by cyclonic eddies (Brzezinski et al., 1998; Siegel et al., 1999), and transport of nutrients and productivity offshore from coastal, frontal or upwelling areas by either cyclonic or anticyclonic eddies (Garcia-Gorriz and Carr, 2001; Lima et al., 2002; Whitney and Robert, 2002). Productivity enhancement due to eddy pumping is generally seen in the centre of upwelling cyclonic eddies and at the periphery of convergent anticyclonic eddies (Mordasova et al., 2002). However, once formed, mesoscale eddies can go through decay phases where the initial upwelling or downwelling is arrested, moderated and/or reversed (Bakun, 2006). The circulation can therefore change dramatically depending on the age and history of the eddy.

Because the nutricline may be depressed by 100 m or more in the centre of an anticyclonic or warm-core (WC) eddy, such eddies have the capacity to reduce primary production. In the long term, with both light (Shiomoto et al., 1998) and water-column stability (Froneman et al., 1999) important controls on production, WC eddies can develop ecosystems with low biomass and a community composed of small cells able to effectively compete for recycled nutrients (Li and Dickie, 1985; Landry et al., 1998; Burkill et al., 1993).

The Haida WC eddies in the NE Pacific actually enhance local primary production rates both by transporting nutrient-rich water offshore, and by enhancing production rates in central eddy water (Crawford et al., 2005). Investigators noted that the deep centre of a WC eddy can be an important reservoir of both micro- and macro-nutrients for phytoplankton growth. This means that in anticyclonic features, production of phytoplankton such as diatoms can be enhanced, at least in the short term, by nutrient enrichment including important inputs of iron from coastal waters (Peterson et al., 2005). WC eddies interacting with the continental shelf also have been seen to generate what Cresswell (1994) calls “slope intrusions” of nutrient-rich water on to the continental shelf in the East Australian Current; such mechanisms have highlighted the importance of WC eddies for fisheries such as the gemfish off eastern Australia (Prince and Griffin, 2001).

Cold-core (CC) eddies, on the other hand, usually increase nutrient supply to the euphotic zone because the nutricline is raised. These nutrient increases are sometimes limited to depths immediately below the mixed layer in Gulf Stream rings (Vaillancourt et al., 2003). In subtropical areas and mid-latitude Atlantic waters, CC eddies can be responsible for ~30% of the total nitrate flux into the euphotic zone (Oschlies and Garçon, 1998). The introduction of new nutrients would be expected *a priori* to support populations of large phytoplankton cells including diatoms (McGillicuddy and Robinson, 1997). This in turn would be fuel for higher trophic levels, since large fractions of primary production in these systems can be grazed (Froneman and Perissinotto, 1996).

Mesoscale eddies may play an important role in nutrient transport and productivity enhancement off the coast of Western Australia (WA) (Feng et al., 2007). Sources of surface nutrient supply driving marine productivity off WA are of special regional interest, since the coast supports the Western Rock Lobster fishery, whose larvae spend 9–11 months in the open ocean off the continental shelf before they settle closer to shore (Caputi et al., 2003). Because the Leeuwin Current (LC) transports surface waters poleward, suppressing upwelling that would otherwise supply surface nutrients and enhance productivity in these regions, the WA coast is very low in nutrients (Pearce, 1991). In such waters, the formation of large, long-lived LC eddies may have a significant impact on both local and regional productivity patterns.

LC eddies are unique among those formed in eastern boundary currents in that they are the only significant features formed by a warm current along the continental slope, and this is the only region where many WC and CC eddies are formed together. Very few LC eddies have been deliberately transected by oceanographers, so relatively little is known about their influence on the regional biogeochemistry and ecology. SeaWiFS ocean-colour imagery suggests that anticyclonic eddies of the LC have higher near-surface concentrations of chlorophyll *a* than adjacent waters, and that the time of maximum concentration is mid-winter, when the LC is most intense (Griffin et al., 2001). Cresswell and Griffin (2004), however, found a local fluorescence minimum in the center of an anticyclonic LC eddy south of our study region.

Our study investigates production patterns in two counter-rotating mesoscale eddies formed in

May 2003, about 5–6 months after their generation. To address the question of whether these particular eddies are typical for the study region, we first present analysis of the history of mesoscale eddy formation over the last 11 years, as determined by satellite altimeter estimates of sea-level anomaly. We then provide an analysis of the dissolved inorganic nutrient uptake and productivity patterns within the two eddies, and hypothesize as to what might be the key factors controlling their productivity.

## 2. Methods

### 2.1. Satellite altimetry

Synoptic maps of sea-surface height anomaly (SSHA) were estimated on a  $0.2^\circ \times 0.2^\circ$  grid, at 4-day intervals for 1993–2003, using all available satellite altimeter (ERS-1 and 2, Envisat, Topex/Poseidon, Jason-1 and Geosat Follow-On) and coastal tidegauge observations, by optimal interpolation methods essentially the same as those of Griffin et al. (2001). To find and track individual eddies from birth to disappearance within the region  $21\text{--}38^\circ\text{S}$ ,  $103\text{--}117^\circ\text{E}$ , we first computed the local sea-level anomaly LSLA (equal to SSHA minus the instantaneous spatial average across the region) then found all extreme points with  $\text{LSSHA} > 15$  cm or  $\text{LSSHA} < -15$  cm. Sea-level features that could be recognized repeatedly for more than 60 d were interpreted as being the signatures of significant individual WC or CC mesoscale eddies, typically 100–200 km in diameter. This process yielded a dataset indicating how many eddies were created each year, at what time and place, as well as their strength (as represented by SSHA), trajectory and lifetime.

### 2.2. Eddies 2003 research voyage

In October 2003, we undertook a 23-day research voyage to investigate the physical, chemical and biological dynamics of two counter-rotating mesoscale eddies of the LC off the coast of WA, formed in May 2003. The evolution of the eddy field was monitored by satellite radar altimetry and radiometry (sea-surface temperature (AVHRR) and ocean colour) for several months before the cruise, and promising features were followed to ascertain their appropriateness for study. The primary criteria were (1) that the eddy features occur between the Abrolhos Islands and Cape Leeuwin, our proposed

area of study, and (2) that the eddies be mature, and reasonably distinct from surrounding waters. The two features identified for study by September 2003 were a pair of counter-rotating WC and CC eddies  $\sim 150$  km off the coast. Such pairs are known as eddy dipoles (Feng et al., 2007).

#### 2.2.1. Cruise track and station locations

We occupied a total of 98 sampling stations within the two eddies over 23 days (Fig. 2), using a set of diagonal transects. Station-sampling transects alternated with underway transects during which we towed the SeaSoar, an underwater sampler containing a high-resolution conductivity temperature and depth (CTD) sensors and a fluorometer to measure chlorophyll *a* fluorescence. While towed, the SeaSoar oscillated between two prescribed depths separated by up to 200 m. We alternated between surface tows ( $\sim 0\text{--}200$  m) and tows in which we attempted to resolve what we considered at the time to be the density gradient marking the bottom boundary of the eddies (e.g.,  $\sim 200\text{--}400$  m for the WC eddy). Sampling started in the WC eddy (October 1–12, 2003) and then proceeded to the CC eddy (October 13–23, 2003).

Because the aim was to characterize the two eddies radially, we targeted stations considered to be representative of the eddy centre (C), body (B) and perimeter (P) on each transect. These were later converted to distance from eddy centre for each station (distances for each region are summarized in Table 1). Positions of moving eddy centres were calculated based on Gaussian fits to the altimeter SSHA data as detailed elsewhere (Feng et al., 2007). A single pass through an eddy consisted of three stations, nominally C, B, and P, of which at least one station involved full assessment of primary production (Production Stations, see below), followed by a full-diameter (ca. 12-hour) SeaSoar run through the eddy. Post-cruise data were sorted by distance from the eddy centre where the eddy centre was adjusted for movement. Due to time constraints some SeaSoar transects resolved only one eddy boundary. During all transects, we used an Acoustic Doppler Current Profiler (ADCP) to measure current strength and direction down to  $\sim 300$  m. The ADCP was also used to locate the eddy centre (below).

#### 2.2.2. Water sampling

Sampling at each station consisted of a cast to 500 m using a conductivity, temperature and depth

Table 1  
**Eddies '03: Summary of eddy chemistry and biology for production stations (experimental stations for production and nutrient uptake estimates)**

Production and experimental stations	Distance from eddy centre (km) (SD)	MX depth (m) (SD)	[SiO <sub>4</sub> ] (μmol)	[NO <sub>3</sub> ] (μmol)	[PO <sub>4</sub> ] (μmol)	Chl <i>a</i> biomass (mg m <sup>-3</sup> )	Ratio large/total Chl <i>a</i> biomass (%)	Total particulate primary prod. (mg C m <sup>-3</sup> d <sup>-1</sup> )	Ratio large/total particulate primary prod. (%)	Particulate organic carbon (total) (mg C m <sup>-3</sup> )	Microzooplankton biomass (mg C m <sup>-3</sup> )	Macrozooplankton biomass* (D = day; N = night) (mg C m <sup>-3</sup> )	Larval fish biomass <sup>§</sup> (mg C m <sup>-3</sup> )
<b>Warm core</b>													
Centre													
BK	5 (2)		0.68	0.05 (0)	0.12 (0.00)	0.37	13	2.25	24	70.0	1.49	9.59 (1.38) D	2.96 (3.28)
MX	67 (26)		0.82 (0.12)	0.05 (0)	0.11 (0.00)	0.40	14	3.90	23	67.2	1.40	4.94 (0.74) N	
BK	65 (14)		0.71	0.05 (0)	0.09 (0.00)	0.24	37	2.83	14	129.3	1.49	N/A	4.42 (5.17)
MX	50 (20)		0.72 (0.00)	0.05 (0)	0.09 (0.00)	0.20	8	3.09	23	44.0	1.79	N/A	
Body													
BK (J)	64 (4)		N/A	0.05 (0)	N/A	0.22	11	1.14	15	59.4			
0 m (J)			2.07	0.05 (0)	0.11	0.17	11	1.14	15				
MX (J)	70 (17)		0.99	0.15	0.08	0.20	21	1.50	18	87.29			
Perim													
BK	118 (4)		0.54	0.05	0.14	0.24	4	3.94	12	86.79	2.92	1.89 (0.54) D	5.75 (3.77)
MX	90 (22)		0.33 (0.19)	0.13 (0.15)	0.16 (0.02)	0.63	15	5.04	14	63.14	3.67	4.48 (0.26) N	
Mean WC													
Cold core													
Centre													
BK	5 (2)		N/A	N/A	0.09 (0.02)	0.07	1	1.24	3	46.19	1.70	1.56 (0.89) D	6.32 (3.32)
MX	106 (9)		1.48 (0.09)	0.18 (0.25)	0.12 (0.02)	0.50	1	2.52	1	39.40	0.80	2.97 (1.43) N	
Body													
BK	37 (12)		N/A	0.05 (0)	N/A	0.10	2	1.39	6	56.26	1.00	N/A	12.77 (3.99)
MX	115 (20)		1.42 (0.27)	0.42 (0.81)	0.13 (0.07)	0.34	11	1.31	2	55.93	0.30	N/A	
Perim													
BK	68 (10)		1.80	0.05	0.06	0.08	2	1.30	4	43.16	3.50	1.03 (0.30) D	7.43 (4.34)
MX	101 (12)		1.23 (0.17)	0.35 (0.29)	0.13 (0.03)	0.55	2	2.02	2	54.89	0.80	5.16 (0.73) N	

These are a subset of all stations, for which data are summarized in Table 2. Centre, body and perimeter denote sets of stations with increasing distance from eddy centre (see text for details). “J” denotes stations within the warm surface jet (WSJ) between the eddies. Means are given with standard deviations (SD). \* See Strzelecki et al. (2007), for details. §See Muhling et al. (2007), for details.

probe (Seabird SBE 911 CTD) mounted on a 24-bottle rosette. Light was measured using a Licor LI-192SA sensor, and chlorophyll *a* fluorescence was traced continuously with a Chelsea Aquatrack-a<sup>TM</sup> fluorometer. Water samples were taken at ~15 depths, with 10 depths concentrated in the mixed layer (mixed-layer depths were ~70 m for CC eddy; ~270 m for the WC eddy) and further sampling every 50–100 m to 500 m. Generic sampling at all depths included unfiltered nutrient samples for nitrate, phosphate, silicate and ammonium, and two size fractions of chlorophyll *a* (mixed layer only). Nitrate, nitrite, silicate and phosphate analyses were performed using Quik-Chem<sup>TM</sup> methods on a flow injection LACHAT<sup>®</sup> instrument using the following protocols: for nitrate and/or nitrite we used Quik-Chem<sup>TM</sup> Method 31-107-04-1-A; detection limit ~0.03  $\mu\text{mol L}^{-1}$  (adapted from Wood et al., 1967; a detection limit of 0.05  $\mu\text{mol L}^{-1}$  was used in this study). For silicate analyses, we used Quik-Chem<sup>TM</sup> Method 31-114-27-1-D; limit of detection ~0.05  $\mu\text{mol L}^{-1}$  (adapted from Murphy and Riley, 1962), and for phosphate: Quik-Chem<sup>TM</sup> Method 31-115-01-1-G; limit of detection ~0.02  $\mu\text{mol L}^{-1}$  (adapted from Armstrong, 1951). Ammonium concentrations were determined using a technique developed by Kerouel and Aminot (1997) and adapted for flow injection by Watson et al. (2004).

For production stations, two depths were sampled more intensively, the surface, which was sampled by hand-held bucket (BK), and the chlorophyll maximum as selected from fluorescence trace during the down cast (MX). Samples were also taken at five depths for assessment of primary production via <sup>14</sup>C in two size fractions (large > 5  $\mu\text{m}$  and small < 5  $\mu\text{m}$ ; see Section 2.2.3). Depths were chosen to represent a light gradient for primary production including at least one sample within the deep chlorophyll *a* maximum and one below it. Nutrient uptake was measured as the uptake of <sup>15</sup>NO<sub>3</sub><sup>-</sup> or <sup>15</sup>NH<sub>4</sub><sup>+</sup> in two size fractions, total phytoplankton and large phytoplankton (> 5  $\mu\text{m}$ ), in BK and MX samples (Section 2.2.4).

For chlorophyll *a*, 1 L was gently vacuum filtered on to a GF/F for total (TOT) and 2 L were filtered on to a nominally ~5- $\mu\text{m}$  Nitex screen (L for large, or > 5  $\mu\text{m}$ ). These were immediately extracted in 90% acetone overnight for analysis on board using a Turner Designs T400 fluorometer. For high performance liquid chromatography (HPLC) analyses, 4-L samples were filtered on to GF/F filters

(nominal porosity of 0.7- $\mu\text{m}$ ) from each BK and MX depth. Analyses were executed with Waters<sup>®</sup> instrumentation (a Waters 996 Photodiode Array Detector, a Waters 600 Controller, and a Waters 717plus Autosampler). The HPLC system used an SGE 250\*4.6 mm SS Exsil ODS (octadecyl silica) 5- $\mu\text{m}$  column. Pigments were eluted over a 30 min period with a flow rate of 1 mL min<sup>-1</sup>. The gradient used follows Wright et al. (1991): (1) 80:20 (v/v) methanol:ammonium acetate buffer 0.5 mol L<sup>-1</sup> pH of 7.2; (2) 90:10 (v/v) acetonitrile:MilliQ water; (3) 100% ethyl acetate. Each solvent was pre-filtered through a Millipore HVLP 0.45- $\mu\text{m}$  filter. The separated pigments were detected at 436 nm and identified against standard spectra using Empower<sup>TM</sup> software. Concentrations of the pigments were determined from standard (Sigma and purified pigments obtained from algal cultures).

### 2.2.3. Primary production

Gently-mixed samples were poured into one dark and two clear 140-mL polycarbonate bottles (duplicate experiments) to which 20  $\mu\text{Ci}$  of NaH<sup>14</sup>CO<sub>3</sub> were added. Bottles were incubated on deck from dawn-to-dawn (24 h) in plexiglass tubes covered with a range of blue and neutral films that simulate the intensity and nature of the underwater light field within the euphotic zone. Seawater pumped from ~5 m below surface filled the incubator tubes and flowed continuously under pressure to keep samples at near-surface water temperatures. Incubations were terminated in the dark by pouring the content of each incubation bottle through a 25-mm diameter disk of nylon textile (Nitex<sup>TM</sup> mesh size = 5  $\mu\text{m}$ ) and a Whatman GF/F<sup>TM</sup> filter placed in series. The filters were dropped into separate borosilicate vials and HCl was added on the filters (250  $\mu\text{l}$  of 0.5 N) in order to remove non-incorporated <sup>14</sup>C. Vials were left open in a fume hood overnight or until the HCl had evaporated and the filters were dry. The activity was measured on a LKB RackBeta<sup>TM</sup> after adding 10 ml of scintillation cocktail. Carbon uptake was calculated using a value of 26,900 mg C m<sup>-3</sup> for the concentration of dissolved inorganic carbon.

### 2.2.4. Dissolved inorganic nitrogen (DIN) uptake

Gently-mixed samples were poured into two clear 2.3-L culture-bottles to which trace amounts of K<sup>15</sup>NO<sub>3</sub> (~0.05  $\mu\text{mol L}^{-1}$  final concentration) and H<sub>2</sub><sup>13</sup>CO<sub>3</sub> (~20  $\mu\text{mol L}^{-1}$  final concentration) were added to one bottle, and <sup>15</sup>NH<sub>4</sub>Cl (~0.05  $\mu\text{mol L}^{-1}$

final concentration) and  $\text{H}_2^{13}\text{CO}_3$  ( $\sim 20 \mu\text{mol L}^{-1}$  final concentration) to the other. Bottles were incubated on deck in running seawater tubs under full sunlight for the surface samples and under blue and neutral films to simulate 1% light conditions for deep samples. Incubations were terminated after 6–9 h by pouring the content of each incubation bottle first through a 5- $\mu\text{m}$  nitex mesh and then through pre-combusted (500 °C, 12 h) 25-mm Whatman GF/F<sup>TM</sup> filters under low vacuum ( $< 50 \text{ mmHg}$ ). The contents of the nitex mesh were rinsed on to GF/F filters and all filters were dried at 60 °C then stored over desiccant until analysed by mass spectrometry. Uptake rates were calculated for carbon ( $\rho\text{C}$ ), nitrate ( $\rho\text{NO}_3$ ) and ammonium ( $\rho\text{NH}_4$ ) and total nitrogen uptake ( $\rho\text{N}$ ) is considered as the sum of  $\rho\text{NO}_3$  and  $\rho\text{NH}_4$ , since  $\text{N}_2$  uptake was an order of magnitude lower (Holl et al., 2007).

### 2.3. Calculations and statistical analyses

Biomass and production were integrated by trapezoidal integration over one of two depth intervals: (1) euphotic zone when the deepest sample was 0.1% surface PAR (which was often  $< 110 \text{ m}$ ) at production stations and several non-production stations; (2) 250 m in the case of non-production stations where deep samples were collected. This was done as a first approximation of the chlorophyll *a* biomass in the WC eddy. Chlorophyll *a* in the large ( $> 5 \mu\text{m}$ ) fraction and total chlorophyll *a* were integrated separately prior to calculating the integrated water-column percent contribution by large cells.

We fitted a general linear mixed statistical model (using SPSS) investigating variations in the following variables: total primary production, chlorophyll *a*-specific primary production, nitrate uptake rates, ammonium uptake rates, % production in large ( $> 5 \mu\text{m}$ ) fraction, and the *f*-ratio (*f*-ratio defined as ((nitrate uptake rate + ammonium uptake rate)/total N uptake). Covariates were distance from centre of the eddy, mixed-layer depth (MLD) (m) (defined as a  $\sigma_t$  difference of 0.125 from 10 m; see Feng et al., 2007 for details), sampling depth (m), eddy (WC vs. CC), and size fraction ( $> 5 \mu\text{m}$  vs. total) with random effects involving each station. Two to three outliers were removed from each data set, and data were log-transformed to conform to statistical requirements for homoscedasticity.

## 3. Results

### 3.1. Satellite altimetry

Satellite altimetry can be used to identify and track the intensity of mesoscale eddies over time: WC features appear as positive sea-surface height anomalies, while CC features appear as negative sea-surface heights. Comparing the WC eddy we studied during Eddies 2003 (B03) with all other positive sea-surface height anomalies in the region between 1993 and 2003, it is clear that B03 was a typical large eddy (200 km diameter), with near-equals occurring in 1996, 1998, 1999, 2001 and 2002 (Fig. 1). It is important to note, conversely, that in 1993, 1994, 1995 and 1997, no WC eddies the size of B03 occurred. Turning to the CC eddies, the eddy we investigated during the 2003 Eddies voyage (C03) was the most intense CC eddy of 2003 though it was bettered (but not greatly) in 7 of the 10 previous years. Only 1994, 1997 and 1998 lacked CC eddies as intense as C03. Fig. 1 also shows that the eddies were studied fairly late in their lives, and were just past their peak amplitude, which occurred closer to the middle of the year. Note that we also include, for comparison, an earlier large WC eddy studied by Moore et al. (2007) in 2000 (A00) (Fig. 2).

### 3.2. Eddies 2003 oceanographic overview

The WC and CC eddies sampled during Eddies 2003 were clearly distinct from each other physically and biologically, the WC eddy larger, deeper and more productive ( $p < 0.001$ ; Figs. 3 and 4; Table 1) than the CC eddy. The WC feature had a deep surface-mixed layer as indicated by the plunging  $\sim 25.8 \sigma_t$  density contour, which reached  $\sim 275 \text{ m}$  in the centre of the eddy, where temperatures were above 18 °C (Fig. 3A). Nitrate was undetectable ( $< 0.05 \mu\text{mol L}^{-1}$ ) to 250 m in the WC eddy centre (Tables 1 and 2), and ammonium was undetectable at the surface of the WC eddy ( $< 0.05 \mu\text{mol L}^{-1}$ ) and uniformly below  $0.1 \mu\text{mol L}^{-1}$  within 100 km of the WC eddy centre (data not shown). Fluorescence traces within the WC eddy suggested the presence of a deep and uniform chlorophyll *a* maximum that reached to  $\sim 250 \text{ m}$ ; other fluorescence peaks occurred at the perimeter of the eddy nearer the surface (Fig. 3B).

Nutrient concentrations within the CC eddy indicated that surface nitrate was measurable

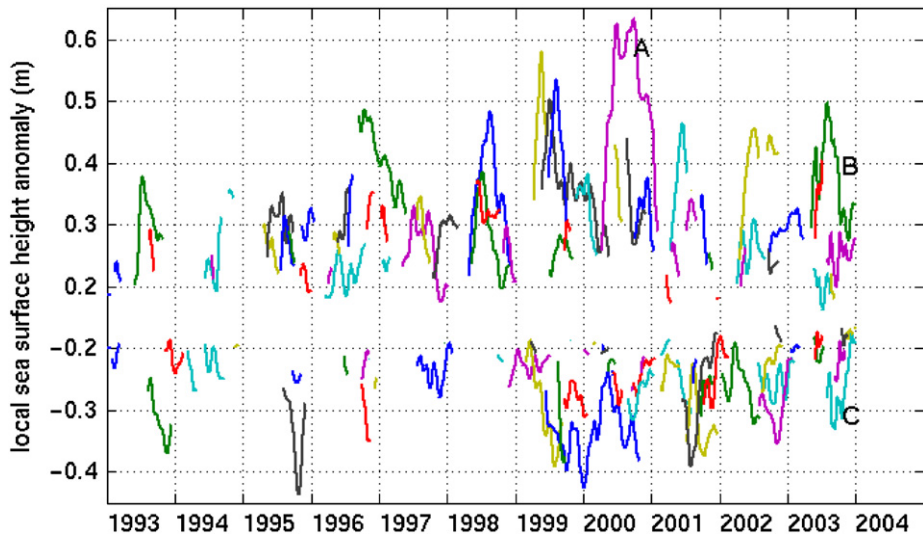


Fig. 1. The time line and intensity of warm-core (positive anomaly) and cold-core (negative anomaly) eddies as central height anomalies in the Leeuwin Current, from birth to disappearance, over the decade before the cruise. Specifically, results are presented for eddies born in the region lat 27–33°S, lon 110–115°E between 1993 and 2003. Label A indicates the eddy studied by Moore et al. in 2000, while Labels B and C indicate the WC and CC eddies, respectively, sampled by Waite et al. in Eddies 2003.

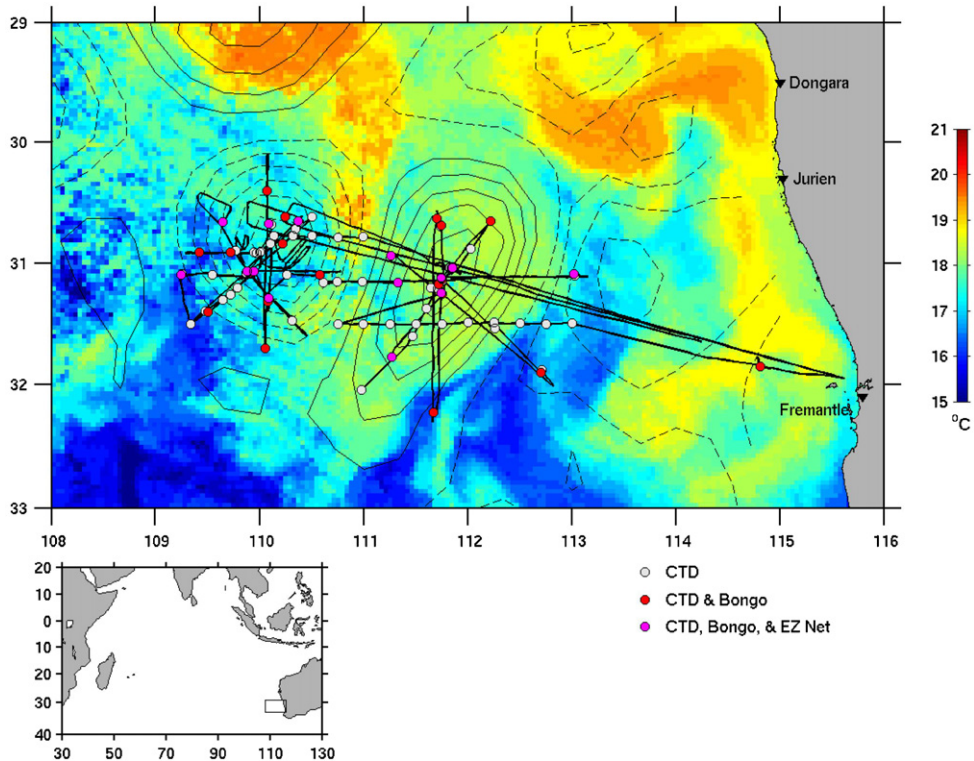


Fig. 2. Ship track showing sampling stations in the WC and CC eddies superimposed on satellite-derived sea-surface temperature for a 3-day composite sea-surface temperature image to 8 October 2003. Solid lines represent positive sea-surface height anomalies (SSHA) including the WC eddy, while dashed lines represent negative SSHA including the CC eddy. White, red and pink circles indicate CTD stations with no nets, bongo nets, and EZ net deployments, respectively (see text for details).

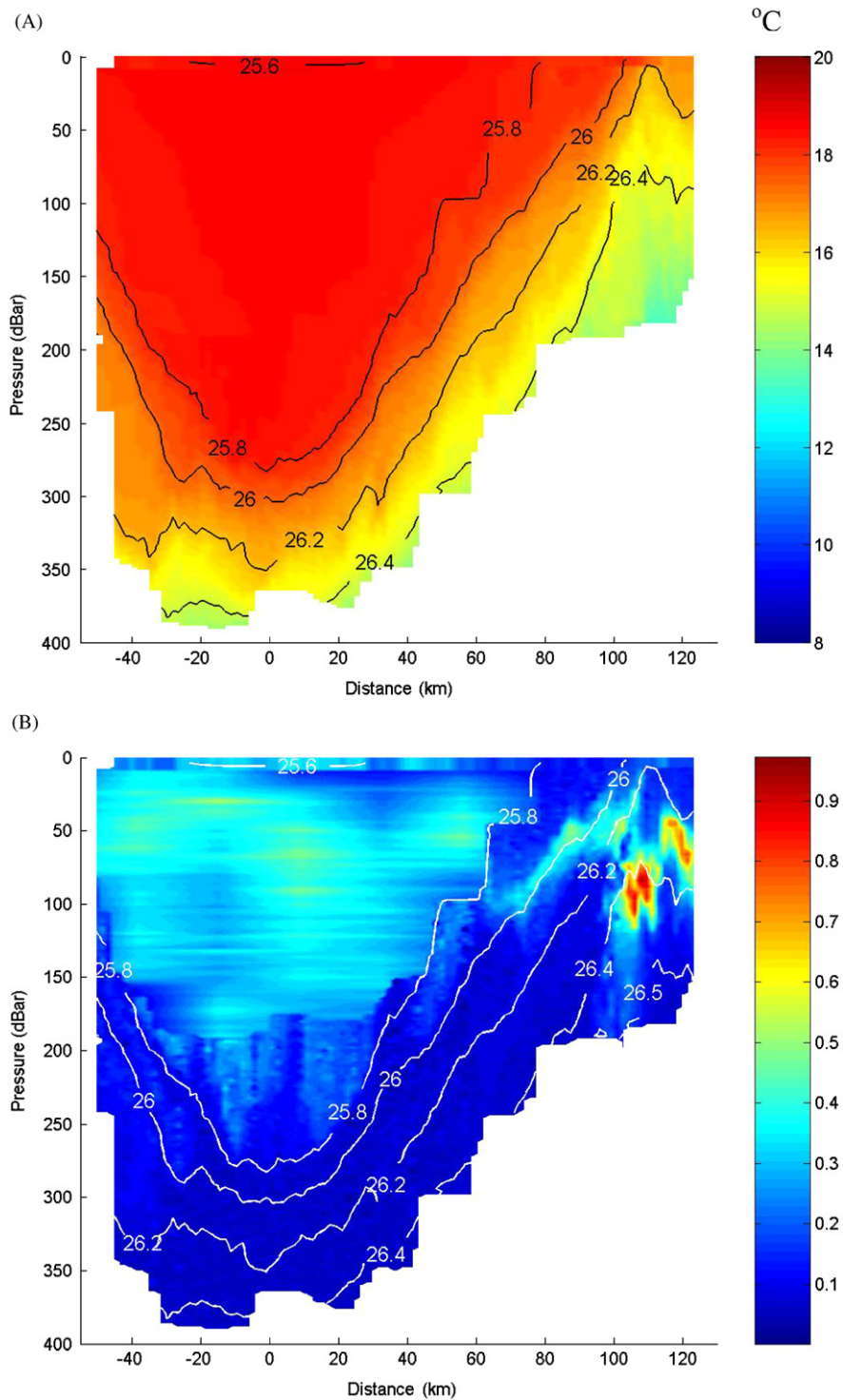


Fig. 3. *Eddies 2003*: SeaSoar transect showing cross section of warm-core eddy with numbered lines denoting density contours as  $\sigma_t$  and distance from eddy centre on X-axis. Colours denote (A) temperature ( $^{\circ}\text{C}$ ) and (B) fluorescence calibrated as  $\text{mg chlorophyll } a \text{ m}^{-3}$ .

(Tables 1 and 2), at  $\sim 0.07 \mu\text{mol L}^{-1}$  in the eddy centre, and ammonium concentrations were substantially higher than in the WC eddy, with a mean

of  $0.24 \mu\text{mol L}^{-1}$  ( $\pm 0.21$ ;  $n = 5$ ) in the eddy centre. The CC eddy showed elevated density contours in the immediate vicinity of the eddy centre, with

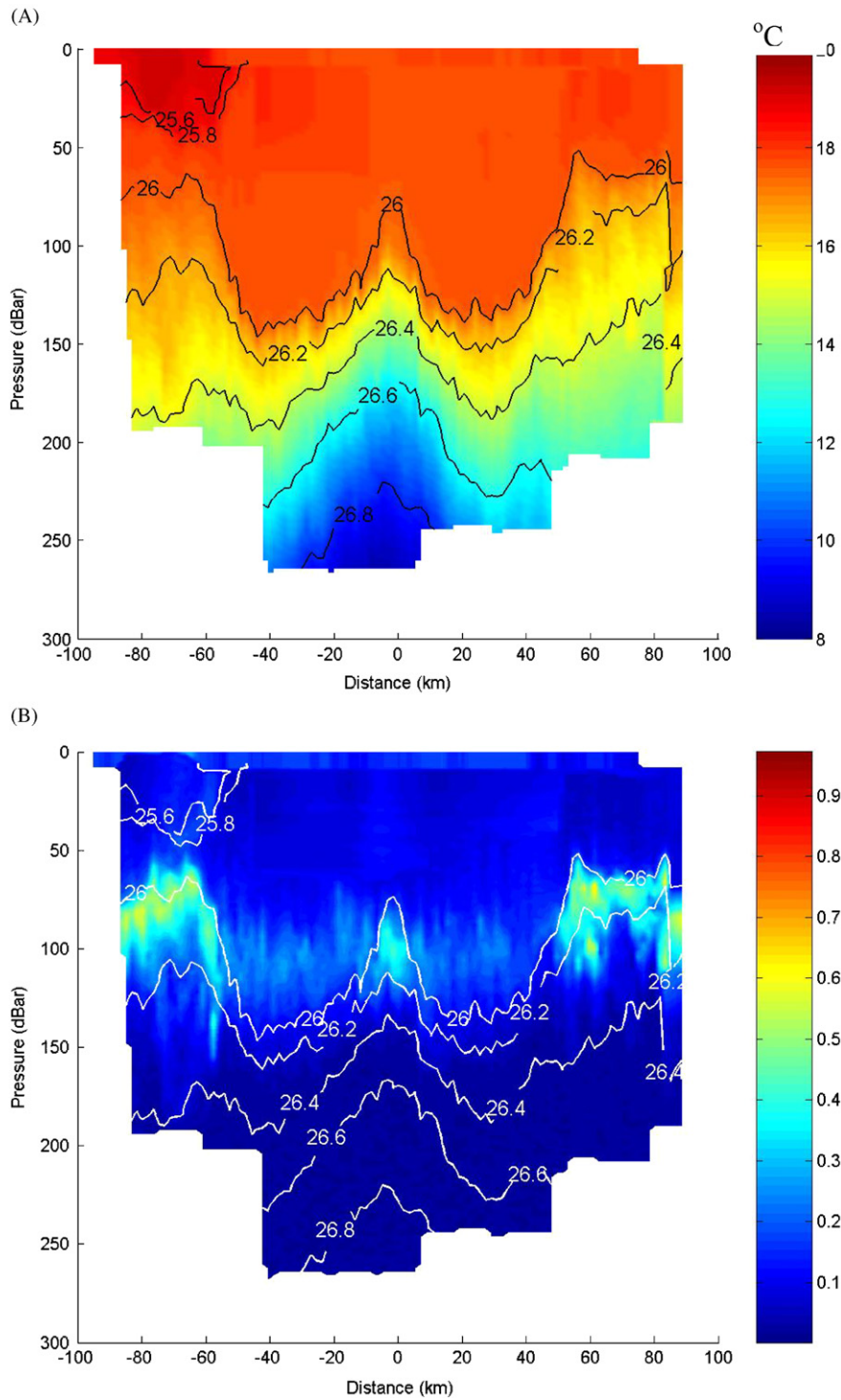


Fig. 4. *Eddies 2003*: SeaSoar transect showing cold-core eddy with numbered lines denoting density contours as  $\sigma_t$  and distance from eddy centre on  $X$ -axis. Colours denote (A) temperature ( $^{\circ}\text{C}$ ) and (B) fluorescence calibrated as  $\text{mg chlorophyll } a \text{ m}^{-3}$ . Note the cap of warm water at eddy surface and fluorescence peaks at the central upwelling node and periphery of the eddy.

Table 2  
*Eddies '03*: Summary of eddy chemistry and biology for all stations

Station	Surface										Integrated					
	Mean distance from eddy centre (km) (SD)	Range of distances from eddy centre (min–max)	Dsi ( $\mu\text{mol}$ ) (SD)	DNO <sub>3</sub> ( $\mu\text{mol}$ ) (SD)	DPO <sub>4</sub> ( $\mu\text{mol}$ ) (SD)	Chl <i>a</i> ( $\text{mg m}^{-3}$ )	Ratio large/total Chl <i>a</i> (%)	Total primary production ( $\text{mg C m}^{-3} \text{ d}^{-1}$ )	Ratio large/total primary production (%)	NO <sub>3</sub> ( $\text{mmol m}^{-2}$ )	PO <sub>4</sub> ( $\text{mmol m}^{-2}$ )	Total chl <i>a</i> biomass ( $\text{mg m}^{-2}$ )	Ratio large/total Chl <i>a</i> biomass (%)	Total primary production ( $\text{mg C m}^{-2} \text{ d}^{-1}$ )	Ratio large/total primary production (%)	
<b>Warm core</b>																
Centre ( <i>n</i> = 8)	13 (4)	8–18	0.65 (0.09)	0.05 (0.00)	0.12 (0.004)	0.19	14	2.57	25	70.0	9.9	40.9	16	484	19	
Body ( <i>n</i> = 8)	60 (10)	41–73	0.95 (0.15)	0.05 (0.00)	0.11 (0.00)	0.27	37	2.83	14	69.6	8.8	38.0	9	263	16	
Perimeter ( <i>n</i> = 9)	101 (18)	75–123	1.31 (1.08)	0.05 (0.00)	0.12 (0.01)	0.22	7	2.82	13	69.4	12.5	34.0	11	407	11	
<b>Cold core</b>																
Centre ( <i>n</i> = 12)	14 (9)	7–41	1.39 (0.13)	0.07 (0.03)	0.09 (0.02)	0.07	1	1.24	3	130.4	12.0	18.5	1	175	3	
Body ( <i>n</i> = 18)	36 (11)	19–48	1.27 (0.18)	0.06 (0.02)	0.09 (0.01)	0.10	2	1.39	6	135.9	10.3	21.4	1	209	4	
Perimeter ( <i>n</i> = 12)	73 (14)	47–105	1.43 (0.21)	0.06 (0.02)	0.08 (0.02)	0.11	2	1.57	4	135.5	10.2	30.3	3	308	5	

isopycnals shoaling to a depth of 75 m (Fig. 4A). There was also direct evidence that the CC eddy was surface-convergent; a mooring released a significant distance away from the eddy centre was retrieved in the exact centre of the eddy 2 weeks later, and the centre of the eddy also had collected a number of drifting buoys and other flotsam. A fluorescence peak occurred at ~100 m in the immediate vicinity of the raised thermocline in the CC eddy centre; this was highly localized and only ~15 km in diameter. This chlorophyll *a* maximum in the centre of the CC eddy was found to be closely associated with the bottom of the mixed-layer (Fig. 4B); on average it was located ~15 m above the MLD (where  $\Delta\sigma_t$  was 0.125). Surface fluorescence was otherwise low overall throughout most of the eddy, but there were fluorescence peaks at 60–80 m around the eddy perimeter (Fig. 4B).

Two other regional oceanographic features are of note in terms of their possible influence on WC and CC eddy dynamics. A large warm (~19 °C) surface water mass to the north of our study region was gradually moving south in the weeks before the cruise. As it approached the eddy dipole, a filament of that water was drawn between the two eddies, forming a feature that we refer to as the warm surface jet (WSJ; Fig. 5). To the south-east of the WC eddy lay a large region of relatively cold (15–16 °C) Subtropical Front Water (SFW) (Fig. 5). While the surface layers of the SFW were actually colder than the surface waters of the CC eddy, the SSHA (measured by altimeters) was only about –20 cm indicating that the surface temperature anomaly did not extend to great depths. However, the SSHA did increase through the period of the cruise suggesting that it was an intensifying feature.

Overall, the regional biological oceanography as represented by the subsurface fluorescence signal was therefore dominated by a series of mesoscale features, visible in the composite SeaSoar trace (Fig. 5): east of the eddies, the Subtropical Front (STF) intruded towards the north, with its distinct deep fluorescence maximum. The WC eddy and the CC eddy were separated by the WSJ; this latter feature had a distinct and shallower fluorescence peak at ~50 m associated with it (Fig. 5). When SeaSoar fluorescence data were calibrated as chlorophyll *a* and integrated to 150 m, the WC feature emerged as the most significant chlorophyll-containing mesoscale feature of the region (Fig. 5), with greater integrated phytoplankton biomass than any

other regional feature. This was confirmed by analytical sampling indicating that WC chlorophyll *a* concentrations were 0.14–0.7  $\mu\text{g L}^{-1}$  vs. 0.06–0.8  $\mu\text{g L}^{-1}$  for the CC eddy, for example (Table 1).

### 3.3. Eddies 2003: biomass, production and nutrient uptake

The WC eddy contained relatively uniform chlorophyll *a* concentrations in a mixed layer much deeper than that found in the CC eddy (Figs. 3 and 5). The lowest chlorophyll *a* concentrations were found at the surface of the CC eddy, while values from the deep chlorophyll *a* maxima were similar to the higher values found in the WC eddy. In general, large phytoplankton cells (>5  $\mu\text{m}$ ) contributed about 15% of phytoplankton biomass (measured as chlorophyll *a*) in the WC eddy, though values varied from 8% to 44%. Microscopic observation indicated these were large diatoms. Large phytoplankton contributed only 1–3% of biomass in the CC eddy (Table 1), significantly less than in the WC eddy (see also Thompson et al., 2007). Large phytoplankton cells in the WC eddy contributed an average of ~16% of primary production, compared to ~4% in the CC eddy (Tables 1 and 3), and % large production had statistically significant trends with depth and distance from eddy (see below and Table 4).

Distinct differences between eddies were apparent when pigments were analysed via HPLC pigment analyses. Here we can see the dominance in the WC eddy of fucoxanthin and diadinoxanthin, pigments associated with diatoms, prymnesiophytes, and crysophytes, while divinyl chlorophyll *a* (DV chl*a*), typical of *Prochlorococcus* spp., was more dominant in the CC eddy (Fig. 6; see also Thompson et al., 2007, for more detail).

Primary production by all phytoplankton (total primary production) in the WC eddy averaged ~2 × that in the CC eddy. Vertically integrated production in the WC eddy was similarly 1.7 × that in the CC eddy (Tables 1–3). When each eddy was considered separately, there was no significant effect of MLD on production rates. Differences in production rates with increasing MLD became significant when data from both eddies were pooled, and were driven by fact that the deepest MLDs occurred only in the WC eddy. It is thus impossible to consider eddy and MLD independently, and we present output from the inter-eddy comparison only (Table 4), and address this matter further in the

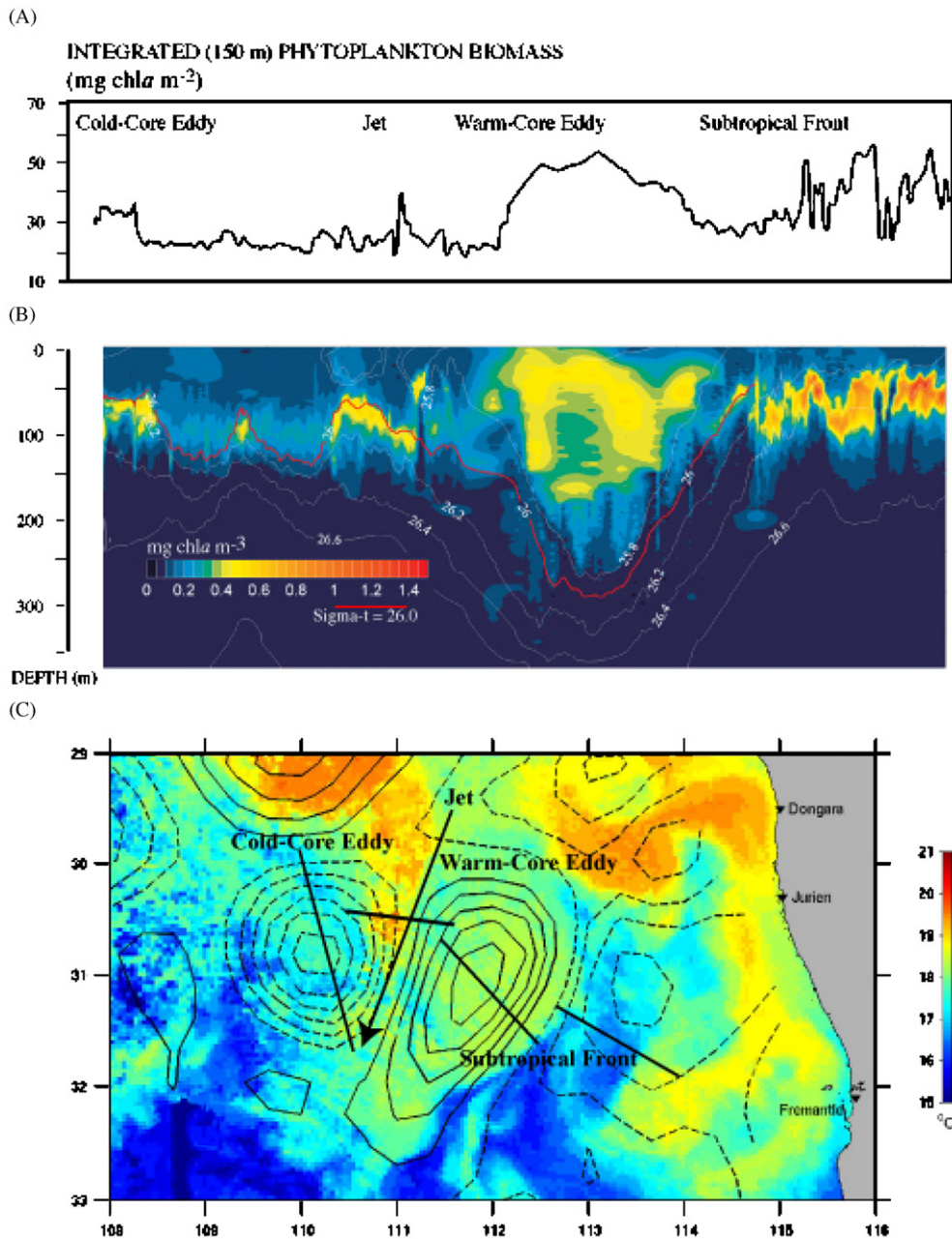


Fig. 5. *Eddies 2003*: (A) Chlorophyll *a* biomass integrated to 150 m as estimated from calibrated fluorescence as seen in (B), a composite of four SeaSoar transects showing regional scale variation of subsurface fluorescence within the cold-core (CC) and warm-core (WC) eddies separated by the warm surface jet (WSJ) generated between the eddies (solid arrow). East of the WC eddy is Subtropical Front Water (SFW), a mild CC feature typified by an intense fluorescence maximum at depth. White lines are isopycnals. Note that the more diffuse layer of chlorophyll *a* in the WC eddy in general contains more vertically integrated chlorophyll *a* biomass than any other regional feature. (C) SeaWiFS sea-surface temperature image as in Fig. 2, showing the location of the CC, WC, WSJ and SFW and the actual ship track for the SeaSoar transects (solid black lines).

Discussion. Chlorophyll *a*-specific production was ~50% higher in the CC eddy than in the WC eddy (Table 3), decreasing with water depth in both eddies, but with a significantly steeper slope in the

CC eddy (Fig. 7; Table 4). Within the WC eddy, there was a significantly greater proportion of production taking place in large cells (> 5 μm) than in the CC eddy, and this proportion also decreased

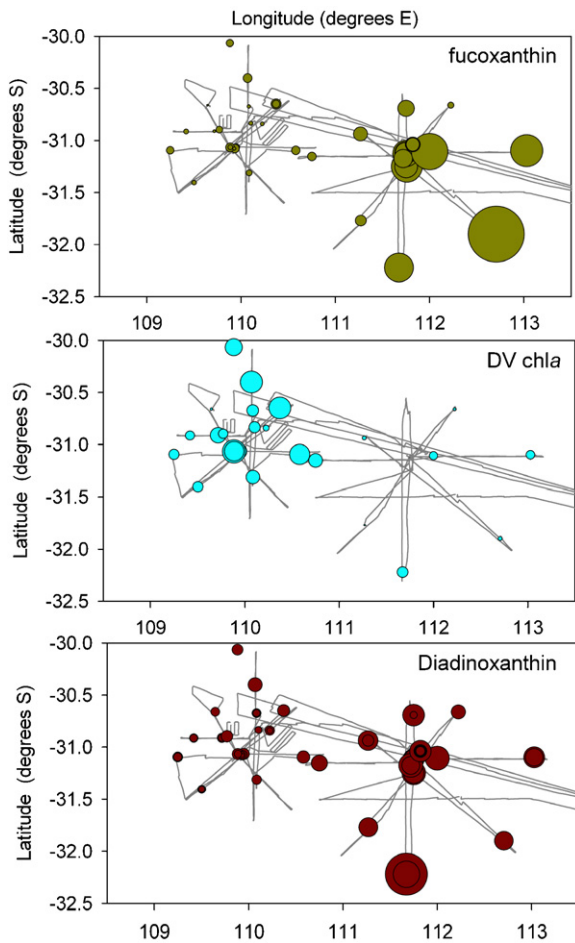


Fig. 6. Pigment concentrations in the cold-core (CC) and warm-core eddy (WC) as analysed by high performance liquid chromatography (HPLC). Bubbles on the cell density plots are proportional to the square root of pigment density: concentrations in  $\mu\text{g L}^{-1}$  (min–max): fucoxanthin (0.004–0.812); divinyl chlorophyll *a* (0.011–0.199); diadinoxanthin (0.003–0.135).

with distance from the centre, especially in the WC eddy (large to total production ratio, Table 4). The large to total production ratio also decreased significantly with depth within the CC, but not the WC eddy (Table 4; Fig. 7).

Ammonium was the primary nitrogen source in both eddies, but was significantly more important in the CC eddy than in the WC eddy (Table 3). Total nitrate uptake rates were about  $4\times$  greater in the WC eddy than in the CC eddy (Table 3), while total ammonium uptake was more than 2 times greater (Table 4) in the CC eddy than the WC eddy. Both nitrate and ammonium uptake rates showed a significant interaction between depth and distance

from eddy centre. For example, near the eddy centre, N uptake rates in the large fraction ( $>5\mu\text{m}$ ) were more uniform in the vertical, while in the outer regions of the eddies, N uptake rates declined more rapidly with depth (Fig. 8). This was also true for the nitrogen uptake in the total phytoplankton (Table 4). There were no independently-resolvable gradients in N uptake with depth or with distance from eddy centre, but there was a significant change in the depth-dependent slope of the uptake rates of nitrate and ammonium in both eddies. This was also true for the nitrogen uptake in the large ( $>5\mu\text{m}$ ) phytoplankton fraction in the WC eddy (Fig. 8).

While the small ( $<5\mu\text{m}$ ) phytoplankton dominated (57–100%) both nitrate and ammonium uptake in both eddies (Table 4), the large ( $>5\mu\text{m}$ ) phytoplankton in the WC eddy were responsible for a much greater fraction of both nitrate uptake ( $\sim 28\%$ ) and ammonium uptake ( $\sim 43\%$ ) than in the CC eddy (undetectable for either nitrate or ammonium). The *f*-ratio, which provides a measure of phytoplankton preference for nitrate over other N sources, was five times greater in the WC than in the CC (Tables 3 and 4). The *f*-ratio was also significantly greater ( $P = 0.04$ , Table 4) in the large phytoplankton fraction than in the total phytoplankton, suggesting that the presence of larger cells was associated with the increased *f*-ratio within the WC eddy.

The mean *f*-ratio in the WC eddy was 0.35, significantly higher (*t*-test,  $p = 0.002$ ) than the *f*-ratio in the CC eddy (0.07) (Table 3). The large ( $>5\mu\text{m}$ ) size fraction of phytoplankton had a significantly higher *f*-ratio than total phytoplankton in the WC eddy (Tables 3 and 4), and the *f*-ratio in the large size fraction increased with distance from centre of the WC eddy, while that in the total fraction decreased with distance from WC centre (distance  $\times$  size fraction interaction, Table 4). There was no detectable nitrogen uptake in the large size fraction of the phytoplankton in the CC eddy, so it was not possible to calculate the *f*-ratio (Table 3; ND = not detectable).

#### 4. Discussion

Recent analysis suggests that dynamic oceanographic processes occurring at the sub-seasonal temporal scale and on the “meso” spatial scale may be the crucial processes regulating production dynamics related to fisheries (Bakun, 2006). Here we present a synoptic analysis of the mechanisms

Table 3

Mean carbon, nitrate and ammonium uptake rates and  $f$ -ratios across the warm-core (WC) and cold-core (CC) eddies, respectively, for total phytoplankton and large phytoplankton ( $> 5 \mu\text{m}$ )

	Warm core eddy			Cold core eddy		
	Mean	Std. error	$n$	Mean	Std. error	$n$
Total primary production ( $\text{mg C m}^{-3} \text{d}^{-1}$ )	4.0	0.31	64	2.0	0.14	73
Total integrated production ( $\text{mg C m}^{-2} \text{d}^{-1}$ )	400	44	11	240	43	13
Chl $a$ -specific production ( $\text{mg C mg Chl } a^{-1} \text{d}^{-1}$ )	12.3	1.04	62	18.2	1.82	65
Large production (%)	16	0.8	64	4	0.3	72
Total $\text{NO}_3$ uptake ( $\text{N mol L}^{-1} \text{h}^{-1}$ )	0.97	0.22	19	0.25	0.05	10
Large $\text{NO}_3$ uptake (%)	27.5	6.1	19	ND	ND	10
Total $\text{NH}_4$ uptake ( $\text{N mol L}^{-1} \text{h}^{-1}$ )	1.78	0.27	19	4.39	0.82	10
Large $\text{NH}_4$ uptake (%)	43.2	10.3	19	ND	ND	10
$f$ -ratio (total)	0.35	0.06	19	0.07	0.02	10
$f$ -ratio (large)	0.48	0.06	19	N/A	N/A	10

Note that N-uptake in the large size fraction within the CC eddy was undetectable (ND) across the 10 experiments executed. Integrations were performed to the 0.1% light depth (see text for details).

underlying production patterns in two mesoscale eddies of the LC off WA, a WC and paired CC eddy. The dynamics of the LC have been implicated in interannual variability in fisheries recruitment (Caputi et al., 2001), but the mechanism driving these correlations is presently unresolved.

#### 4.1. Satellite altimetry

The satellite oceanography indicates that the WC eddy studied in Eddies 2003 by Waite and co-workers (see 13 papers this volume; Eddy B03 in Fig. 1), was a relatively large, long-lived feature. Eddy B03 was very similar in structure and history to Eddy A00 studied by Moore and co-workers (2007), which had the highest local sea-surface height anomaly (LSSHA) documented in the 13-year time series. Few of the other large WC eddies were as long-lived as A00 and B03. In fact, careful inspection of the eddy histories reveals that of all the large WC eddies, the histories of A00 and B03 most resemble those of each other. Both initially formed just off Rottneest Island, A00 in late March, and B03 in late April. Both spent a longer period than most other WC eddies near the continental shelf, and were the southern members of a trio of eddies forming warm-cold-warm triplets. It appears that existing in the triplet makes the southern WC member grow especially large; in both cases the CC eddy in the centre of the triplet (C03 in 2003) eventually looped anticlockwise around the southern WC eddy. In the other years, the dominant eddies formed farther north, more closely resembling the modeled eddies of Rennie et al.

(2007), and/or propagated west more quickly after formation.

What the results of the satellite altimetry analysis mean for the interpretation of the 2003 field programme is that while the basic mechanism of formation of both eddies (mixed barotropic and baroclinic instability of the LC, e.g., Batteen and Butler, 1998; Feng et al., 2005) is the same as for some eddies in all years (i.e. an instability of the LC grows until it pinches off and drifts west), the 2003 cruise (and the 2000 cruise; Moore et al., 2007) sampled slightly rarer WC eddies that were both large and long-lived as a consequence of remaining in contact with the flow of the LC along the continental shelf longer than usual. By the time they were studied, however, both eddies had been out of contact with the LC and the continental shelf for about a month, and hence can both be considered as classical examples of large, mature WC eddies of LC origin. The increased chlorophyll  $a$  concentration in B03 had been visible as high sea-surface chlorophyll in SeaWiFS images from the previous month (September 2003, Feng et al., 2007), which had been distinctive against the lower background surface chlorophyll  $a$  concentrations in the region, and particularly, in comparison to the CC eddy where surface chlorophyll  $a$  was low (Feng et al., 2007). We postulate that the WC eddy B03 had trapped a large volume of LC water (equivalent to several weeks of flow, see Feng et al., 2007) and moved it offshore over the 5–6 month period since formation. The extent to which this LC water represented a nutrient source is explored elsewhere (Greenwood et al., 2007); these authors suggest that

Table 4  
Outcome of tests of fixed effects (eddy, water depth, distance from eddy centre, size fraction) on primary production and nutrient uptake rates, and  $f$ -ratios. Interaction terms shaded in grey

	Distance from eddy centre	Water depth	Size fraction (total vs. > 5 $\mu\text{m}$ )	Eddy	Depth $\times$ eddy	*Distance $\times$ size fraction	<sup>5</sup> Depth $\times$ distance
Total particulate primary production	NS	NS	N/A	$P = 0.0003$ DF = 22			
Chl $a$ -specific production	NS	$P < 0.0001$ DF = 102	N/A	$P = 0.0084$ DF = 21	$P = 0.019$ DF = 102		
Ratio of large to total production (%)	$P = 0.031$ DF = 107	$P < 0.0001^a$ DF = 107	N/A	$P < 0.0001$ DF = 21	$P = 0.0002$ DF = 107		
$f$ -ratio	NS*	NS	NS*	$P = 0.009$ DF = 11		$P = 0.043$ DF = 30	
Nitrate uptake	NS <sup>§</sup>	NS <sup>§</sup>	$P = 0.004$ DF = 29	$P = 0.0090$ DF = 11			$P = 0.0325$ DF = 14
Ammonium uptake	NS* <sup>§</sup>	$P = 0.0009$ DF = 12	$P = 0.0015$ DF = 26	$P = 0.0016$ DF = 13		$P = 0.0114$ DF = 26	$P = 0.0152$ DF = 26

All estimates were executed on log-transformed data. NS = no significant effect.

<sup>a</sup>Note: Primarily a response of the CC eddy—% large production with depth is almost uniform in the WC eddy.

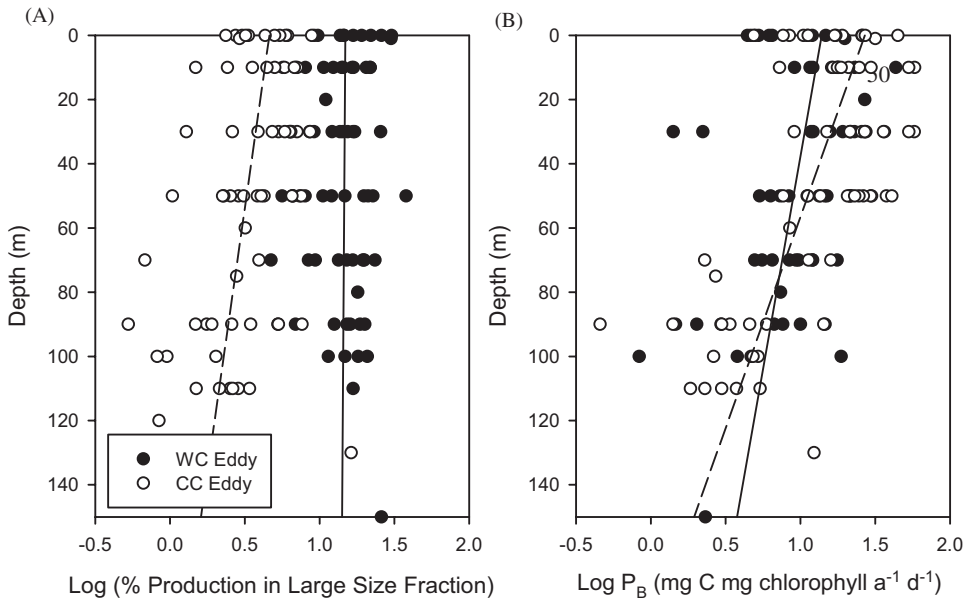


Fig. 7. Depth-specific patterns in primary production within the eddies (all log values). Lines represent statistically significant trends in (A) % production in the large (> 5 μm) size fraction and (B) in chlorophyll *a*-specific production with depth. Note that the WC eddy shows more uniform production with depth, while there are clear decreases with depth within the CC eddy. See also Thompson et al. (2007) for a more detailed discussion.

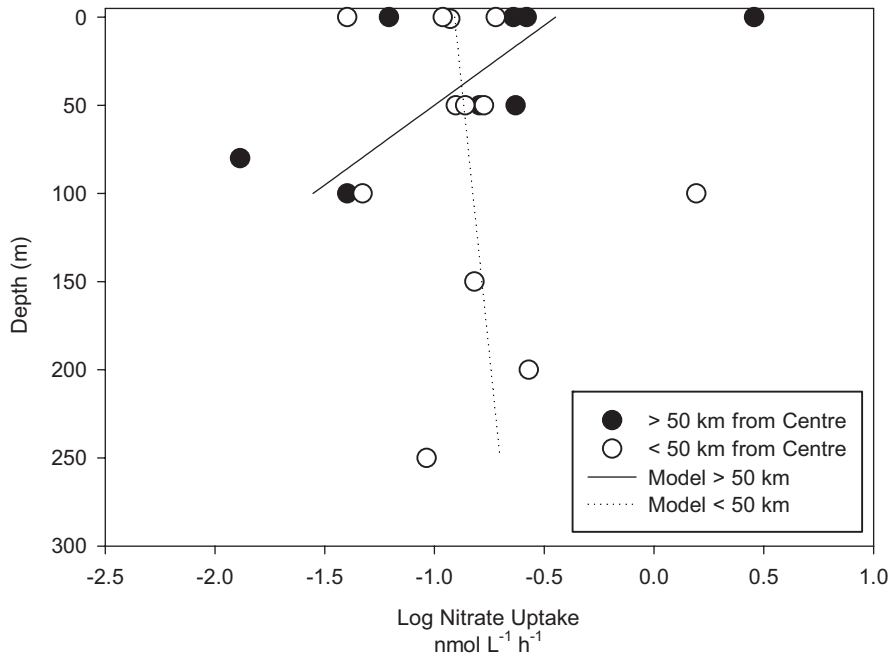


Fig. 8. Nitrate uptake rates in the large (> 5 μm) phytoplankton fraction of the WC eddy only, showing a steepening in the decrease of nitrate uptake with depth, further from the centre of the eddy.

up to 50% of the production in the WC eddy may have been fuelled by nutrients incorporated at the time of eddy formation.

C03, on the other hand, appears to be a more typical example of an intense LC CC eddy that formed seaward of the LC upstream of a developing

LC meander. Was the surface convergence we observed in the CC eddy typical for this current system? CC eddies elsewhere can be a significant source of deep water to the euphotic zone via upwelling and surface divergence in the eddy centre (Vaillancourt et al., 2003), but by the time a CC eddy begins to decay it can become surface convergent (Bakun, 2006). Our observation of clear surface convergence near the centre of C03 might possibly have been related to the early stages of eddy decay, but the eddy was apparently close to its physical peak when sampled (Fig. 1), and a warm cap of water at the surface of C03 seemed to have inhibited the movement of cooler water to the surface, such that C03 may have neither fully upwelled nor become surface divergent (see Fig. 4). Griffin et al. (2001) noted that several satellite-tracked surface drifters became trapped right in the centre of CC eddies in this region, suggesting that surface convergence similar to what we observed may actually be typical of CC eddies formed in this region. This has significant implications for the controls of productivity within the LC system. Rennie et al. (2007) show model results that indicate that such CC eddies may be sourced from the deeper LC Undercurrent, suggesting that what was observed in Eddies 2003 may actually have been typical for LC CC eddies, although we cannot confirm her hypothesis that a meander of the Leeuwin Undercurrent was involved in the process.

#### 4.2. Biomass distributions

In its regional context, the elevated biomass (as integrated chlorophyll *a*) in the WC eddy represented an important mesoscale increase in phytoplankton standing stock, with significant potential to support higher biological productivity including secondary and tertiary production in the ecosystem. In contrast, the CC eddy generally exhibited oligotrophic oceanic conditions by global standards ( $<0.1 \text{ mg Chl } a \text{ m}^{-3}$ ; Antoine et al., 1996), while WC eddy was mesotrophic in comparison to a worldwide survey of open ocean waters ( $0.1\text{--}1 \text{ mg Chl } a \text{ m}^{-3}$ ; Antoine et al., 1996). So although the majority of the WC eddy chlorophyll *a* biomass was in small cells as is typical of oligotrophic systems (see Psarra et al., 2005; Seki et al., 2001), the WC eddy chlorophyll *a* concentrations were higher than other WC eddies in oligotrophic systems such as those found in Mediterranean (Psarra et al., 2005). Where hori-

zontal nutrient gradients are important in determining mesoscale eddy productivity, the distribution of both new production and phytoplankton biomass within an eddy is strongly dependent on the nutrient dynamics at the time of eddy formation (Levy, 2003). The distribution of new production can resemble patterns of vorticity in such cases, and the phytoplankton biomass peak in the eddy centre correlates with surface temperature (Levy, 2003) such that there are radial gradients in biomass and uptake rates. The general correlation (e.g., in the SeaSoar cross-section) between surface temperature and chlorophyll in WC eddy B03 gives support to the notion that the nutrients were incorporated as the eddy formed (see Greenwood et al., 2007 for a modeling test of this hypothesis). In addition, though phytoplankton assemblages in the CC eddy C03 are typical of open ocean assemblages off Australia, the WC eddy assemblage is more similar to those found in waters on the continental shelf (Thompson et al., 2007).

#### 4.3. Primary production

A ring of high-production water on the perimeter of a WC eddy is considered typical of Southern Hemisphere WC eddies (de Souza et al., 2006). This is consistent with the depression of the thermocline in the vortex centre, where cold, nutrient-rich water is displaced downward away from the euphotic zone, decreasing production rates (de Souza et al., 2006). The increase in production rates and biomass in the centre of the WC eddy we studied, apparently a typical LC eddy, is therefore of general interest and suggests that LC eddies are atypical of other WC eddies studied. Our documentation of higher total productivity in the WC eddy than in the CC eddy was further supported by observations of higher nitrate uptake rates and higher *f*-ratios within the WC eddy. The increasing fraction of production in large phytoplankton as the WC eddy centre was approached suggests that the increase in total production in the WC eddy was at least partly a function of greater large phytoplankton biomass, especially diatoms, in the WC eddy. The dependence of increased production on increased diatom biomass would be consistent with the hypothesis above regarding nutrient (including phytoplankton) enrichment at eddy inception being an important factor in determining WC eddy ecology. The increase in WC eddy primary production therefore could be driven both by the historical incorporation

of nutrients and seed populations of diatoms, and by environmental conditions (including a deeper mixed layer) favouring the growth of diatoms relative to other phytoplankton. This is explored more fully in Thompson et al. (2007).

The precise role of MLD in determining the regionally anomalous mesotrophic production levels in the WC eddy remains speculative, since differences in production driven by changes in MLD could not be extracted statistically from inter-eddy differences in MLD. However, our data support the notion that the deep mixing in the centre of the WC eddy consistently increased productivity deep within the eddy—both nitrate and ammonium uptake, and chlorophyll *a*-specific production rates, were higher, deeper, in the centre of the WC eddy, than at the outer radius of the WC eddy or the CC eddy. The peak in production of large phytoplankton in the centre of the WC eddy also supports the notion that the deep MLD of the WC eddy may have favoured the maintenance of a deeply mixed diatom population, consistent with arguments presented by Thompson et al. (2007) that a lower light level favoured the maintenance of diatoms in the centre of the WC eddy. A deep MLD also may have favoured increased ammonium supply via an increase in the regeneration path length (see Section 4.4); this is also consistent with the local peak in ammonium uptake in the WC eddy centre.

The chlorophyll *a*-specific production  $P_B$  was ~50% higher in the CC eddy than in the WC eddy, and  $P_B$  in the CC eddy declined more steeply with depth. Such a depth-dependence could be driven either by shifts in cell physiology such as the chlorophyll *a* quota, or by changes in the carbon fixation rate *per se*. Variation in  $P_B$  is known to be related to phytoplankton acclimation to differences in irradiance or temperature (Geider, 1987) or nutrients (Chalup and Laws, 1990). Temperature differences in the mixed layers between eddies or between the surface and mean MLDs (177 m in the WC eddy and 105 m in the CC eddy) were relatively small, averaging ~1 °C. These are insufficient to shift  $P_B$  or the phytoplankton C:chl *a* ratio significantly (Geider, 1987). Over the average MLDs the mean irradiance was 66% greater in the CC eddy, a difference that could reduce the chlorophyll *a* quota of photoacclimated and nutrient sufficient cells by ~40% and could explain the greater  $P_B$ . The POC:chl *a* ratio was greatest in the surface samples from the CC eddy (Thompson

et al., 2007), an expected consequence of greater  $P_B$ . The greater slope of  $P_B$  vs. depth in the CC eddy is consistent with a reduced rate of vertical mixing in the CC eddy relative to the WC eddy (Thompson et al., 2007). We suggest that phytoplankton in the WC eddy have a chl *a* quota that is determined more by the mean irradiance over the MLD while those in the CC eddy are more fully acclimated to the irradiance at the depth sampled. Such a hypothesis would explain the observed steep slope of  $P_B$  vs. depth in the CC and the intersection at ~80 m. DIN concentrations were sufficiently low that they also may have increased C:chl *a* ratios (Chalup and Laws, 1990) and  $P_B$ . Average MLD DIN (DIN = nitrate + nitrite + ammonium) tended to be greater in the CC eddy than the WC eddy, and, if having an effect, should reduce  $P_B$  in the CC eddy. Therefore we suggest that physiological responses to irradiance > nutrients > temperature are responsible for the rise in  $P_B$  within the CC eddy.

#### 4.4. DIN uptake

Across both eddies and all depths, ammonium dominated as a nitrogen source to phytoplankton, such that *f*-ratios were always <0.5 and <0.1 within the CC eddy. The lack of nitrate uptake and the low *f*-ratio in the CC eddy may be due partly to the greater relative and absolute abundance of prochlorophytes in the CC eddy. DV chl *a* was much more abundant in the CC than the WC eddy (46% of the MV chl *a* in the CC eddy and only 8% of the MV chl *a* in the WC eddy, or six times relatively more abundant; Thompson et al., 2007). Prochlorophytes are the only taxa with DV chl *a* likely to be present in abundance (Chisholm et al., 1992). As prochlorophytes are not likely to be using nitrate (Moore et al., 2002) they can be expected to decrease the *f*-ratio in the CC eddy in the <5 μm and total fraction. The *f*-ratio as calculated here however, does not, give any indication of possible enhanced uptake of N by nutrient-starved phytoplankton (Dugdale et al., 1981; McCarthy, 1981).

Both ammonium and nitrate uptake within the WC eddy peaked in the eddy centre. Greenwood and co-workers (2007) predicted that a deeper mixed layer would increase the time available for regeneration of nutrients (e.g., re-supply of nitrogen as ammonium), increasing production rates overall. In addition, the δ<sup>15</sup>N of particulate organic matter decreased with increasing MLD (Waite et al., 2007),

and the authors present an argument suggesting that this is driven by an increase in ammonium incorporated into phytoplankton as MLD increased.

However, the  $f$ -ratio in the WC eddy for total phytoplankton also peaked in the WC eddy centre. The high nitrate uptake in the WC eddy ( $4 \times$  that of the CC eddy) is of special interest when one considers that the estimated vertical diffusive nitrate flux into the WC eddy was only  $\sim 50\%$  of that estimated for the CC eddy (Greenwood et al., 2007) and Waite et al. (2007) argue that higher  $\delta^{15}\text{N}$  values for phytoplankton overall in the CC eddy suggest an greater relative nitrate availability in that eddy. In this case, it seems likely that the higher  $f$ -ratio could be driven at least partly by the presence of diatoms with a nitrate requirement, which were favoured by the presence of a deep MLD in the centre of the WC eddy. The  $f$ -ratio in the WC eddy was also  $\sim 25\%$  higher in the large ( $> 5\mu\text{m}$ ) size fraction, where diatoms were significant contributors to nitrate uptake. Other processes not quantified in our study such as nitrification could have increased nitrate supply (Wankel et al., 2006).

Results from a 1-D model suggest that incorporation of nutrients at the time of eddy formation could account for up to 50% of the production measured here (Greenwood et al., 2007). In addition, estimated vertical nutrient fluxes along the eddy boundary could account for up to 30% of the daily production rate (Greenwood et al., 2007). However, the high rates of nitrate uptake in the WC eddy, especially in the  $> 5\mu\text{m}$  fraction (Table 3), are consistent with the presence of still further additional nitrate sources. There was isotopic evidence that the diatom population accessed nutrient sources which were distinct from those used by the  $< 5\mu\text{m}$  cells and which were more typical of deep nitrate sources (Waite et al., 2007). We speculate that the high  $f$ -ratios in the WC eddy are likely to be supported by nitrate injections from a range of other sources, with anecdotal evidence supporting three possible mechanisms: (1) isopycnal mixing, (2) entrainment from the WSJ between the two eddies, and/or (3) lateral injections of nitrate from nutrient-rich water masses such as the SFW to the southeast. For example, salinity anomalies near the base of the pycnocline suggest earlier intrusion of waters surrounding the WC eddy via isopycnal mixing may have occurred, but the magnitude is unclear (M. Feng, pers. comm.). Nutrient concentrations in waters beneath the WSJ are some of the highest in

the surface waters of the region, but the time scale of their possible entrainment into the eddy is unclear (S. Pesant, unpubl. data). Process measurements at the chlorophyll  $a$  maximum at the SE perimeter of the WC eddy suggest that mixing might have been occurring at depth with SFW (Paterson et al., 2007), a hypothesis supported by hydrodynamic analysis (Feng et al., 2007). However the relative magnitude of these additional sources was beyond the scope of our analysis.

#### 4.5. Heterotrophy

Nutrient injections into heterotrophic systems with high turnover and well-developed bacterial populations can be very rapidly cycled into the microbial loop (Krom et al., 2005), such that nutrient supply into such systems cannot be simply parameterized as increases in production rates (Psarra et al., 2005). Both eddies we studied were overall highly heterotrophic. Microzooplankton herbivory was a key feature of both the WC and the CC eddies, possibly controlling not only picoplankton production and abundance but also mediating diatom production in the WC eddy (Paterson et al., 2007), with the WC having more predatory dinoflagellates than ciliates in the mix of predators (i.e. predators capable of targeting the large phytoplankton fraction). We therefore expect nutrient recycling to be a key factor determining overall production rates, and a key factor enhancing production in the WC eddy.

This primary production in the WC eddy seemed to be available to higher trophic levels: mesozooplankton were twice as abundant in the WC eddy as in the CC eddy, at  $\sim 100$  individuals  $\text{m}^{-3}$  in the WC eddy (Strzelecki et al., 2007; Table 1), consistent with observed differences in phytoplankton abundance between the eddies. Though the abundance of the zooplankton in the eddies was much lower than was generally observed in the LC/continental slope environment (Strzelecki et al., 2007), both the increased abundance of herbivores (Strzelecki et al., 2007) and their superior physiological state (Waite et al., 2007) suggest an enhanced “classic” food web within the WC eddy in comparison to the CC eddy.

## 5. Summary

The WC eddies studied in Eddies 2003 and in 2000 by Moore et al. (2007), were long-lived and

large features compared to typical WC eddies, and were similar to each other. Both were generated off Rottneest Island, spent a relatively long time near the coast after generation (~1–2 months), and were mature when sampled. Eddies 2003 sampled a pair of counter-rotating eddies (eddy dipole) with distinct physics and plankton ecology. The WC eddy was elevated in phytoplankton biomass and production, especially in the large (>5 µm) size fraction, which was characterized by chain-forming diatoms in a large phytoplankton fraction with a high *f*-ratio (0.48). The CC eddy contained relatively more prochlorophytes, a much greater portion of the pigments were found at ~100 m and volumetric chlorophyll *a*-specific production ( $P_B$ ) was greater. Our analysis supports the notion that the higher production rates in the WC eddy were a consequence of elevated phytoplankton biomass generated earlier in the eddy's history, and partly dependent on the population of diatoms favoured by the lower light levels in the WC eddy's deep mixed layer. A deeper MLD also seemed associated with increases in nutrient regeneration supporting higher production rates.

Nitrate was probably the nutrient limiting biomass production and was non-detectable to 275 m in the centre of the WC eddy. We suggest that in addition to cross-pycnocline diffusion of nitrate, some lateral sources are likely to have been mixed into the WC eddy if we are to account for the eddy's relatively high rates of nitrate uptake.

### Acknowledgements

We thank the captain and crew of the SS *Southern Surveyor* (Eddies '03) without whose support we could not have tracked the eddies. Eddies '03 was supported by the University of Western Australia, the Faculty of Engineering, Computing and Mathematics (UWA) Strategic Fund, and the Waite et al. Collaborative Project from the Strategic Research Fund for the Marine Environment (SRFME). We thank H. Paterson for the contribution of her picoplankton data, J. Strzelecki for the biomass estimates of the mesozooplankton and B. Muhling for fish biomass estimates. M. Feng provided the estimates of moving eddy centre positions to which we normalized all station locations. We thank the following agencies for ancillary environmental data: (1) Sealevel: Topex/Poseidon & Jason—NASA/CNES, Envisat—ESA, Geosat Follow-On—NOAA, coastal tidegauges—National Tidal Centre (CBoM),

WA Dept of Transport, (2) Sea surface temperature—NOAA and NASA, (3) MODIS Ocean colour—NASA, and (4) Surface drifters—Global Lagrangian Drifter Program. Near real-time and delayed-mode analyses of these data were performed by C. Rathbone (SST) and M. Cahill (sea level and currents) of CSIRO as part of the Bluelink project. The AVISO near-real time altimetry products were also used for planning the voyage.

### References

- Antoine, D., Andre, J.-M., Morel, A., 1996. Oceanic primary production 2. Estimation at global scale from satellite (coastal zone color scanner) chlorophyll. *Global Biogeochemistry* 10 (4), 57–69.
- Armstrong, F.A.J., 1951. The determination of silicate in sea water. *Journal of the Marine Biological Association of the United Kingdom* 30, 149–160.
- Bakun, A., 2006. Fronts and eddies as key structures in the habitat of marine fish larvae: opportunity, adaptive response and competitive advantage. *Scientia Marina* 70S2, 105–122.
- Batteen, M.L., Butler, C.L., 1998. Modeling studies of the Leeuwin Current off Western and Southern Australia. *Journal of Physical Oceanography* 28, 2199–2221.
- Brzezinski, M.A., Villareal, T.A., Lipschultz, F., 1998. Silica production and the contribution of diatoms to new and primary production in the central North Pacific. *Marine Ecology Progress Series* 167, 89–104.
- Burkill, P.H., Edwards, E.S., John, A.W.G., Sleight, M.A., 1993. Microzooplankton and their herbivorous activity in the North Eastern Atlantic Ocean. *Deep-Sea Research II* 40, 479–493.
- Caputi, N., Chubb, C.F., Pearce, A.F., 2001. Environmental effects on the recruitment of the western rock lobster, *Panulirus cygnus*. *Marine and Freshwater Research* 52 (8), 1167–1174.
- Caputi, N., Chubb, C., Melville-Smith, R., Pearce, A., Griffin, D., 2003. Review of relationships between life history stages of the western rock lobster, *Panulirus cygnus*, in Western Australia. *Fisheries Research* 65, 47–61.
- Chalup, M.S., Laws, E.A., 1990. A test of the assumptions and predictions of recent microalgal growth-models with the marine phytoplankter *Pavlova-lutheri*. *Limnology and Oceanography* 35 (3), 583–596.
- Chisholm, S.W., Frankel, S.L., Goericke, R., Olson, R.J., Palenik, B., Waterbury, J.B., West-Johnsrud, L., Zettler, E.R., 1992. *Prochlorococcus marinus* nov. gen. nov. sp.: an oxyphototroph marine prokaryote containing divinyl chlorophyll *a* and *b*. *Archives of Microbiology* 157, 297–300.
- Crawford, W.R., Brickley, P.J., Peterson, T.D., Thomas, A.C., 2005. Impact of Haida eddies on chlorophyll distribution in the Eastern Gulf of Alaska. *Deep-Sea Research II* 52, 975–989.
- Cresswell, G., 1994. Nutrient enrichment of the Sydney continental shelf. *Australian Journal of Marine and Freshwater Research* 45, 677–691.
- Cresswell, G.R., Griffin, D.A., 2004. The Leeuwin Current, eddies, and sub-Antarctic waters off south-western Australia. *Marine and Freshwater Research* 55, 267–276.

- de Souza, R.B., Mata, M.M., Garcia, C.A.E., Kampel, M., Oliveira, E.N., Lorenzetti, J.A., 2006. Multi-sensor satellite and in situ measurements of a warm core ocean eddy south of the Brazil-Malvinas Confluence region. *Remote Sensing of Environment* 100, 52–66.
- Dugdale, R.C., Jones, B.H., MacIsaac, J.J., Goering, J.J., 1981. Adaptation of Nutrient Assimilation, pp. 234–250. In: Platt, T. (Ed.), *Physiological Bases for Phytoplankton Ecology*. Canadian Bulletin of Fisheries and Aquatic Sciences, 210:346p.
- Feng, M., Wijffels, S., Godfrey, J.S., Meyers, G., 2005. Do eddies play a role in the momentum balance of the Leeuwin Current? *Journal of Physical Oceanography* 35 (6), 964–975.
- Feng, M., Majewski, L.J., Fandry, C.B., Waite, A.M., 2007. Characteristics of two counter-rotating eddies in the Leeuwin Current system off the Western Australian coast. *Deep-Sea Research II*, doi:10.1016/j.dsr2.2006.11.022.
- Froneman, P.W., Perissinotto, R., 1996. Structure and grazing of the microzooplankton communities of the Subtropical Convergence and a warm-core eddy in the Atlantic sector of the Southern Ocean. *Marine Ecology Progress Series* 135, 237–245.
- Froneman, P.W., McQuaid, C.D., Laubscher, P.K., 1999. Size-fractionated studies in the vicinity of the subtropical front on an adjacent WC eddy south of Africa in austral winter. *Journal of Plankton Research* 21, 2019–2035.
- Garcia-Goriz, E., Carr, M.E., 2001. Physical controls of phytoplankton distributions in the Alboran Sea: a numerical and satellite approach. *Journal of Geophysical Research—Oceans* 106 (C8), 16795–16805.
- Garcon, V.C., Oeschlies, A., Doney, S.C., McGillicuddy, D., Waniek, J., 2001. The role of mesoscale variability on plankton dynamics in the North Atlantic. *Deep-Sea Research II—Topical Studies in Oceanography* 48 (10), 2199–2226.
- Geider, R.J., 1987. Light and temperature dependence of the carbon to chlorophyll ratio in microalgae and cyanobacteria: implications for physiology and growth of phytoplankton. *New Phytologist* 106, 1–34.
- Greenwood, J.E., Feng, M., Waite, A.M., 2007. A one-dimensional simulation of biological production in two contrasting mesoscale eddies in the south eastern Indian Ocean. *Deep-Sea Research II*, doi:10.1016/j.dsr2.2006.10.004.
- Griffin, D.A., Wilkin, J.L., Chubb, C.F., Pearce, A.F., Caputi, N., 2001. Ocean currents and the larval phase of Australian western rock lobster, *Panulirus cygnus*. *Marine and Freshwater Research* 52, 1187–1199.
- Holl, C., Waite, A.M., Pesant, S., Thompson, P.A., Montoya, J., 2007. Unicellular diazotrophy as a source of nitrogen to Leeuwin Current coastal eddies. *Deep-Sea Research II*.
- Kerouel, R., Aminot, A., 1997. Fluorometric determination of ammonia in sea and estuarine waters by direct segmented flow analysis. *Marine Chemistry* 57, 265–275.
- Krom, M.D., Thingstad, T.F., Brenner, S., Carbo, P., drakopoulos, P., Fileman, T.W., Flaten, G.A.F., Groom, S., Herut, B., Kitidis, V., Kress, N., Law, C.S., Liddicoat, M.I., Mantoura, R.F.C., Pasternak, A., Pitta, P., Polychonaki, T., Psarra, S., Rassoulzadegan, F., Sjkoldal, E.F., Spyres, G., Tanaka, T., Tselepidis, A., Wassmann, P., Wexels Riser, C., Woodward, E.M.S., Zodiatis, G., Zohary, T., 2005. Summary and overview of the CYCLOPS P addition Lagrangian experiment in the Eastern Mediterranean. *Deep-Sea Research II* 52, 3090–3108.
- Landry, M.R., Brown, S.L., Campbell, L., Constantinou, J., Liu, H., 1998. Spatial patterns in phytoplankton growth and microzooplankton grazing in the Arabian Sea during monsoon forcing. *Deep-Sea Research II* 45, 2368–2523.
- Letelier, R.M., Karl, D.M., Abbott, M.R., Flament, P., Freilich, M., Lukas, R., Strub, T., 2000. Role of late winter mesoscale events in the biogeochemical variability of the upper water column of the North Pacific Subtropical Gyre. *Journal of Geophysical Research—Oceans* 105 (C12), 28723–28739.
- Levy, M., 2003. Mesoscale variability of phytoplankton and of new production: impact of the large-scale nutrient distribution. *Journal of Geophysical Research—Oceans* 108 (C11), Art. No. 3358 NOV 22 2003.
- Li, W.K.W., Dickie, P.M., 1985. Growth of bacteria in seawater filtered through 0.2 μm nuclepore membranes: implications for dilution experiments. *Marine Ecology Progress Series* 85, 245–252.
- Lima, I.D., Olson, D.B., Doney, S.C., 2002. Intrinsic dynamics and stability properties of size-structured ecosystem models. *Journal of Geophysical Research—Oceans* 107(C8), Art. No. 3111.
- McCarthy, J.J., 1981. The kinetics of nutrient utilization, pp. 211–233. In: Platt, T. (Ed.), *Physiological Bases for Phytoplankton Ecology*. Canadian Bulletin of Fisheries and Aquatic Sciences 210:346p.
- McGillicuddy, D.J., Robinson, A.R., 1997. Eddy-induced nutrient supply and new production in the Sargasso Sea. *Deep-Sea Research I* 44, 1427–1450.
- Moore, L.R., Post, A.F., Rocap, G., Chisholm, S.W., 2002. Utilization of different nitrogen sources by the marine cyanobacteria *Prochlorococcus* and *Synechococcus*. *Limnology and Oceanography* 47, 989–996.
- Moore II, T.S., Matear, R.J., Marra, J., Clementson, L., 2007. Phytoplankton variability off the Western Australian Coast: mesoscale eddies and their role in cross-shelf exchange. *Deep-Sea Research II*, this issue [doi:10.1016/j.dsr2.2007.02.006].
- Mordasova, N.V., Arzhanova, N.V., Sapozhnikov, V.V., 2002. Influence of eddies on the distribution of nutrients and chlorophyll in the northeastern part of the Black Sea. *Oceanology* 42 (4), 487–493.
- Muhling, B.A., Beckley, L.E., Olivar, M.P., 2007. Ichthyoplankton assemblage structure in two meso-scale Leeuwin Current eddies, eastern Indian Ocean. *Deep-Sea Research II*, doi:10.1016/j.dsr2.2006.05.045.
- Murphy, J., Riley, J.P., 1962. A modified single-solution for the determination of phosphate in natural waters. *Analytica Chimica Acta* 27, 31–36.
- Oeschlies, A., Garcon, V., 1998. Eddy induced enhancement of primary production in a model of the North Atlantic Ocean. *Nature* 394, 266–269.
- Paterson, H.L., Knott, B., Waite, A.M., 2007. Microzooplankton community structure, and herbivory on phytoplankton, in an eddy pair in the Indian Ocean off Western Australia. *Deep-Sea Research II*, this issue [doi:10.1016/j.dsr2.2006.12.011].
- Pearce, A.F., 1991. Eastern boundary currents of the southern hemisphere. *Proceedings of the Royal Society of Western Australia* 74, 35–46.
- Peterson, T.D., Whitney, F.A., Harrison, P.J., 2005. Macronutrient dynamics in an anticyclonic mesoscale eddy in the Gulf of Alaska. *Deep-Sea Research II* 52, 909–932.
- Prince, J.D., Griffin, D.A., 2001. Spawning dynamics of the eastern gemfish (*Rexea solandri*) in relation to regional

- oceanography in south-eastern Australia. *Marine and Freshwater Research* 52 (4), 611–622.
- Psarra, S., Zohary, T., Krom, M.D., Mantoura, R.F.C., Polychronaki, T., Stambler, N., Tanaka, T., Tselepides, A., Thingstad, T.F., 2005. Phytoplankton response to a Lagrangian phosphate addition in the Levantine Sea (Eastern Mediterranean). *Deep-Sea Research II* 52, 2944–2960.
- Rennie, S., Pattiaratchi, C.P., McCauley, R., 2007. Dynamics of the surface and sub-surface currents of south-western Australia: a numerical study. *Deep-Sea Research* 11.
- Seki, M.P., Polovina, J.J., Brainard, R.E., Bidigare, R.R., Leonard, C.L., Foley, D.G., 2001. Biological enhancement of cyclonic eddies tracked with GOES thermal imagery in Hawaiian Waters. *Geophysical Research Letters* 28 (8), 1583–1586.
- Shiomoto, A., Kawaguchi, S., Imai, K., Tsuruga, Y., 1998. *Chla*-specific productivity of picophytoplankton not higher than that of larger phytoplankton off the South Shetland Islands in summer. *Polar Biology* 19 (5), 361–364.
- Siegel, D.A., McGillicuddy, D.J., Fields, E.A., 1999. Mesoscale eddies, satellite altimetry, and new production in the Sargasso Sea. *Journal of Geophysical Research—Oceans* 104 (C6), 13359–13379.
- Strzelecki, J., Koslow, T., Waite, A.M., 2007. Comparison of mesozooplankton communities from a pair of warm- and cold-core eddies off the coast of Western Australia. *Deep-Sea Research II*, doi:10.1016/j.dsr2.2007.02.004.
- Thompson, P.A., Pesant, S., Waite, A.M., 2007. Contrasting the vertical differences in the phytoplankton biology of a dipole pair of eddies in the south-eastern Indian Ocean. *Deep-Sea Research II*, doi:10.1016/j.dsr2.2006.12.009.
- Vaillancourt, R.D., Marra, J., Seki, M.P., Parsons, M.L., Bidigare, R.R., 2003. Impact of a cyclonic eddy on phytoplankton community structure and photosynthetic competency in the subtropical North Pacific Ocean. *Deep-Sea Research Part I* 50 (7), 829–847.
- Waite, A.M., Muhling, B., Holl, C., Beckley, L.E., Montoya, J., Strzelecki, J., Thompson, P.A., Pesant, S., 2007. Food web structure in two counter-rotating eddies based on  $\delta^{15}\text{N}$  and  $\delta^{13}\text{C}$  isotopic analyses. *Deep-Sea Research II*, doi:10.1016/j.dsr2.2006.12.010.
- Wankel, S.D., Kendall, C., Francis, C.A., Payton, A., 2006. Nitrogen sources and cycling in the San Francisco Bay estuary: a nitrate dual isotopic composition approach. *Limnology and Oceanography* 51, 1654–1664.
- Watson, R.J., Butler, E.C.V., Clementson, L.A., Berry, K.M., 2004. Flow-injection analysis with fluorescence detection of trace levels of ammonium in seawater. *Journal of Environmental Monitoring* 7, 37–42.
- Whitney, F., Robert, M., 2002. Structure of Haida Eddies and their transport of nutrient from coastal margins into the NE Pacific Ocean. *Journal of Oceanography* 58, 715–723.
- Wood, E.D., Armstrong, F.A.J., Richards, F.A., 1967. Determination of nitrate in sea water by cadmium-copper reduction to nitrite. *Journal of the Marine Biology Association of the United Kingdom* 47, 23–31.
- Wright, S.W., Jeffrey, S.W., Manoura, R.F.C., Llewellyn, C.A., Bjornland, T., Repeta, D., Welschmeyer, N., 1991. Improved HPLC method for the analysis of chlorophylls and carotenoids from marine phytoplankton. *Marine Ecology Progress Series* 77, 183–196.